

Prediction of precipitate evolution and martensite transformation in Ti-Ni-Cu shape memory alloys by computational thermodynamics

A Povoden-Karadeniz¹, D C Cirstea², E Kozeschnik¹

¹Vienna University of Technology – Institute of materials science and technology, Vienna, Austria

²National Institute for Research and Development in Electrical Engineering INCDIE ICPE-CA, Advanced Materials Department, Bucharest, Romania

E-mail: erwin.povoden-karadeniz@tuwien.ac.at

Abstract. Ti-50Ni to Ti-55Ni (at.%) can be termed as the pioneer of shape memory alloys (SMA). Intermetallic precipitates play an important role for strengthening. Their influence on the start temperature of the martensitic transformation is a crucial property for the shape memory effect. Efforts for increasing the martensite start temperature include replacement of a part of Ni atoms by Cu. The influence of Cu-addition to Ti-Ni SMA on *T₀*-temperatures and the character of the austenite-martensite transformation is evaluated using a new thermodynamic database for the Ti-Ni-system extended by Cu. Trends of precipitation of intermetallic phases are simulated by combining the assessed thermodynamics of the Ti-Ni-Cu system with assessed diffusion mobility data and kinetic models, as implemented in the solid-state transformation software MatCalc and are presented in the form of time-temperature-precipitation diagrams. Thermodynamic equilibrium considerations, complemented by predictive thermo-kinetic precipitation simulation, facilitates SMA alloy design and definition of optimized aging conditions.

1. Introduction

Cold-forged Ti-Ni alloys close to Ti50Ni50 (at.%) have a martensitic B19' structure and transform thermo-elastically to their original austenitic B2-phase during re-heating [1,2]. Precipitation of intermetallic phases during special aging strengthens the shape memory alloy (SMA) [2-5]. Addition of Cu to Ti50Ni50 can stabilize the additional B19-phase at low temperatures, associated with a two-step transformation from austenite to B19' martensite via B19-phase [6-8]. Direct transformation of B2-phase to B19 martensite at higher Cu-contents showed significantly narrowed hysteresis [7].

However, the reported critical Cu-content limiting the single-stage from the two-stage the transformation characteristics is quite scattering. Heat-treated Ti50Ni50-*x*Cu_x showed fine, nano-sized distributions of Cu-containing intermetallic phase of the type Ti(Cu,Ni)₂ inside the grains [8,9].

However, the understanding of the effect of this phase on the transformation behaviour and the knowledge of required Cu-alloying to provoke its precipitation is scarce. Thermodynamic CALPHAD analysis [10,11] constrains the important parameters for transformation and precipitation, namely the critical Cu-content for two-step transformation and the thermodynamic stability of intermetallic precipitate phases theoretically. Povoden-Karadeniz et al. [12] established a thermodynamic Ti-Ni SMA database, containing the metastable precipitate phases Ti₃Ni₄ and Ti₂Ni₃ additionally to the



thermodynamic equilibrium phases of the Ti-Ni system. Two thermodynamic assessments of the Ti-Ni-Cu system are available [13,14], with two different descriptions of the austenitic B2-phase. Tang's [13] assessment focused on the SMA-relevant martensite phases and does not contain model parameters of the ternary Ti(Cu,Ni)₂ solid solution. On the other hand, Zhang's assessment [14] lacks the low-temperature martensite phases, but comprises a comprehensive descriptions of all observed high-temperature phases [15] of the Ti-Ni-Cu system. In our present reassessment of thermodynamic model parameters, we aimed on merging these "partial" assessment to one consistent set of optimized model descriptions which allows computational thermodynamics calculations for all phases of the Ti-Ni-Cu system. In a computational thermo-kinetic evaluation of temperature- and aging time-dependent precipitation in Cu-alloyed Ti-Ni SMA, the assessed thermodynamics are combined with kinetic models for diffusion, nucleation and growth of precipitates, as implemented in the solid-state transformation software Matcalc [16].

2. Computational methods

2.1. Thermodynamic re-optimisation of model parameters

The Ti-Ni-Cu system contains ternary extensions of binary alloy and intermetallic phases, listed in Table 1. Their proposed structural CALPHAD model descriptions [14] were maintained. The use of SMA Ti-Ni database [12] in the Ti-Ni-Cu extension however required some re-adjustments of binary Ti-Cu parameters. For re-optimized Gibbs energies of their ternary extensions, also revised interaction parameters were added to the constitutive Ti-Ni [14], Ti-Cu [17] and Cu-Ni [18] end-member parameters. Model parameters of Tau1 to 6 [14] are ternary phases that are not constituted of stable binary end-member compounds were also re-optimized. These re-adjustments, listed in Table 1, were necessary to merge previous partial assessments to a consistent database of the whole Ti-Ni-Cu system.

Table 1. Re-assessed model parameters of phases in the Ti-Ni-Cu system

| Phase | Model type | Model formula | Parameter | Optimised values |
|---------------------------------|------------------------|---|-----------------|--|
| fcc | Solution ^{a)} | (Cu,Ni,Ti)Va | 0L(Cu,Ni,Ti:Va) | -200000+25T |
| B2 | Ordering ^{b)} | (Cu,Ni,Ti) _{0.5} (Cu,Ni,Ti) _{0.5} (Va) ₃ | Cu:Ti:Va | -7000 |
| | | | Ti:Cu:Va | -7000 |
| | | | 0L(Cu,Ni:Va) | -3000-3T |
| | | | 0L(*:Cu,Ni:Va) | -3000-3T |
| | | | 0L(*:Cu,Ti:Va) | +7000 |
| | | | 0L(Cu,Ti:Va) | +7000 |
| TiCu | CEF | (Cu,Ni,Ti)(Cu,Ni,Ti) | Cu:Ti | G(Cu) ^{a)} +G(Ti)-19000+3.6T |
| | | | 0L(Cu,Ni:Ti) | -83000+19.8T |
| Ti ₂ Cu | CEF | (Cu,Ni)(Ti) ₂ | 0L(Cu,Ni:Ti) | -15000 |
| TiCu ₂ | CEF | (Cu,Ni) ₂ (Ti) | 0L(Cu,Ni:Ti) | -30000 |
| Ti ₂ Cu ₃ | CEF | (Cu,Ni) ₃ (Ti) ₂ | 0L(Cu,Ni:Ti) | -65000 |
| Ti ₃ Cu ₄ | CEF | (Cu,Ni) ₄ (Ti) ₃ | 0L(Cu,Ni:Ti) | -120000-6.7T |
| TiNi ₃ | CEF | (Cu,Ni,Ti)(Cu,Ni,Ti) ₃ | 0L(Cu,Ni:Ti) | -18000 |
| Ti ₂ Ni | CEF | (Cu,Ni,Ti) ₂ (Cu,Ni,Ti) ₁ | 0L(Cu,Ni:Ti) | -18000 |
| | | | 0L(Ti:Cu,Ni) | -15000 |
| | | | 1L(Ti:Cu,Ni) | +15000 |
| | | | 2L(Ti:Cu,Ni) | -15000 |
| Tau1 | CEF | (Cu,Ni) ₂ (Ti) | Cu:Ti | 2G(Cu)+G(Ti)-25000+11T |
| | | | Ni:Ti | 2G(Ni)+G(Ti)-95820-T |
| | | | 0L(Cu,Ni:Ti) | -54500 |
| Tau2 | CEF | Cu _{0.175} Ni _{2.825} Ti ₂ | Cu:Ni:Ti | 0.175G(Cu)+2.825G(Ni)+2G(Ti)-180250+7.2T |
| Tau4 | CEF | Cu _{0.05} Ni _{0.7} Ti _{0.25} | Cu:Ni:Ti | 0.05G(Cu)+0.7G(Ni)+0.25G(Ti)-35500 |
| Tau6 | CEF | Cu _{0.25} Ni _{0.5} Ti _{0.25} | Cu:Ni:Ti | 0.25G(Cu)+0.5G(Ni)+0.25G(Ti)-25000-3.5T |
| B19' | CEF | (Cu,Ni,Ti) _{0.5} (Cu,Ni,Va) _{0.5} | Cu:Ni | 0.5G(Cu-bcc)+0.5G(Ni)+20000 |
| | | | Ti:Cu | 0.5G(Cu-bcc)+0.5G(Ti-bcc)-3900+15T |
| B19 | CEF | (Cu,Ni,Ti) _{0.5} (Cu,Ni,Va) _{0.5} | Ti:Cu | 0.5G(Cu-bcc)+0.5G(Ti-bcc)-7400+T |
| Liquid | Solution | (Cu,Ni,Ti) | Cu,Ti | -19330+7.3T |

^{a)}Regular solution model, ^{b)}Split model of ordering [19], ^{c)}* denotes Cu,Ti or Ni, ^{d)}Gibbs energies of elements adopted from Dinsdale [20]

2.2 Thermo-kinetic precipitation simulation

A thermo-kinetic simulation of the precipitate evolution in Ti-Ni SMA and Ti-Ni SMA alloyed by Cu was performed with MatCalc [16]. The physical modeling base implemented in MatCalc is schematized in Figure 1. It comprises the formalisms of nucleation theory [21], the SFFK model for the growth of precipitates [22] and takes into account CALPHAD-assessed [10, 11] thermodynamic and diffusion mobility data stored in the assessed Ti-Ni-Cu Matcalc databases mc-sma.tdb and mc.sma.ddb supplemented to this paper.

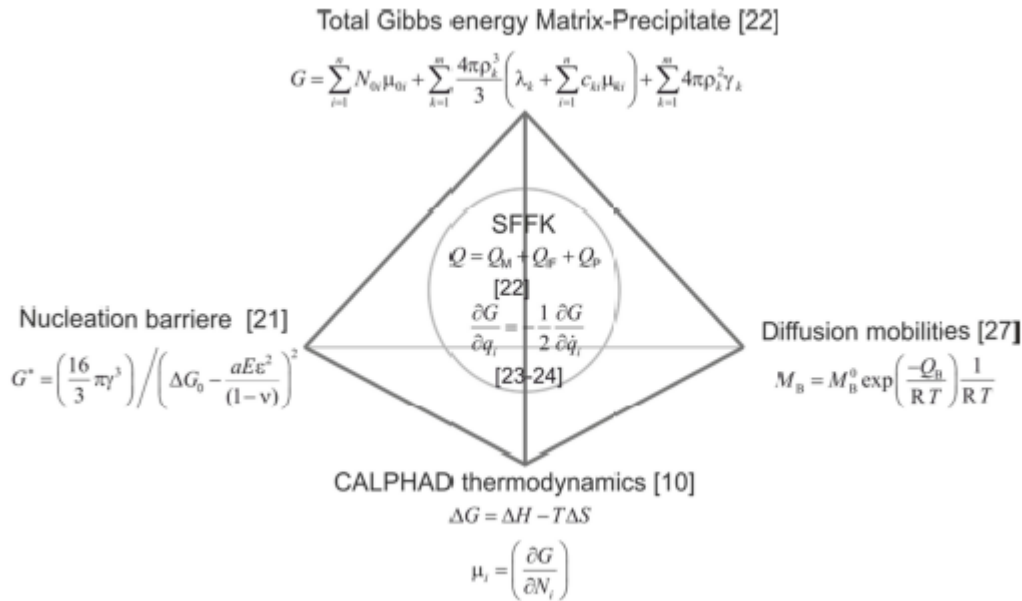


Figure 1. Schematized physical fundament for the precipitation simulation with MatCalc

The rate of radius change and chemical composition change of each precipitate is evaluated by application of the thermodynamic extremum principle [23-25]. Real matrix-precipitate systems are typically in a highly non-equilibrated state and they have thus a high driving force to evolve towards minimum energy state as a function of time and temperature. In the SFFK model three parts contribute to the energy dissipation during the system evolution. These are dissipation due to diffusion inside of the precipitation matrix, dissipation due to interface migration and dissipation due to diffusion inside of the precipitates. In order to evaluate the energy dissipation diffusivity data are thus required. Diffusivities in the matrix are stored in the form of a diffusion mobilities database. Diffusion mobilities contain activities for the diffusion and a pre-factor which basically represents the jump frequency of a solute atom. The diffusivities inside of precipitates were roughly related to the diffusivity in the matrix by a factor of 1/100. The numerical of the evolution equations were presented by Svoboda et al. [22] and Kozeschnik [26].

2.3. Assessment of diffusion mobilities in B2-ordered austenite matrix

For the definition of diffusion mobilities in the B2-ordered austenite matrix phase the modeling of activation energy Q for the diffusivity as suggested by Helander and Agren [27] was followed

$$Q = Q^{\text{dis}} + \Delta Q^{\text{ord}} \quad (1)$$

where dis stands for disordered bcc-phase, i.e. the “parent” reference phase from which the thermodynamics of B2-phase is derived by CALPHAD model parameters describing chemical ordering [19] and ΔQ^{ord} thus denotes a contribution to the activation energy from chemical ordering

with

$$\Delta Q^{\text{ord}} = \sum_i \sum_{j \neq i} \Delta Q_{ij}^{\text{ord}} [y_i^a y_j^b - x_i x_j] \quad (2)$$

x_i is the mole fraction of component I and y_i^a is the atomic fraction of component I on the crystallographic a sublattice sites of the B2-phase.

3. Result and discussion

3.1. Equilibrium thermodynamics of the Ti-Ni-Cu system

As shown in the isothermal section of Figure 2 (a) satisfactory reproduction of experimental high-temperature phase equilibria is obtained with our re-assessed database.

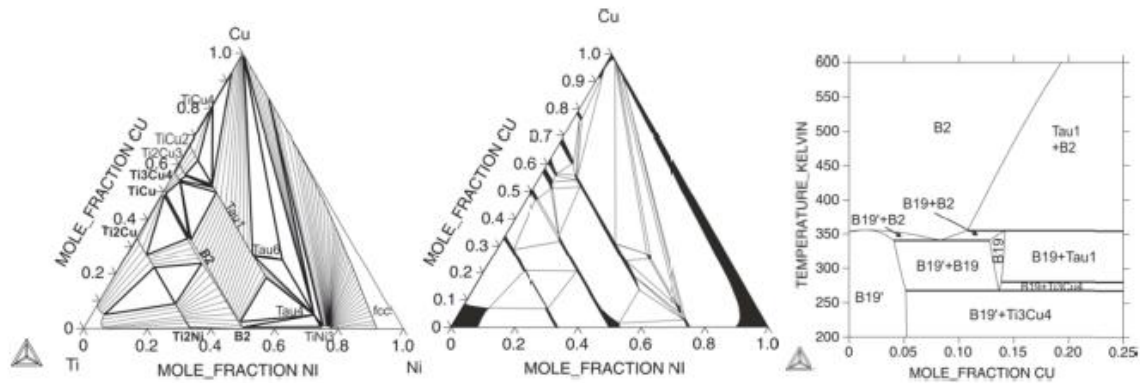


Figure 2. Calculated Ti-Ni-Cu equilibrium phase diagram (a) at 1143 K compared to experiments [15] (b) and (c) calculated Ti-Ni SMA equilibrium phase diagram with varying Cu-content, a small amount of Ti_2Ni is present in all phase regions of Fig.2 (c)

Figure 2 (c) shows the calculated equilibrium phase transformations among martensitic phases at low temperatures. The sequence of stable phase from low to high Cu-content goes along with the observed transformation sequence $\text{B19}' - \text{B19}' + \text{B19} - \text{B19}$. Our calculation suggests $x(\text{Cu}) > 0.14$ for the transition from two-step martensite formation to single B19 martensite.

3.2. Diffusivities in austenitic SMA matrix

In Figure 3 optimized diffusivities of Ti and Ni in B2-austenite are compared with experimental data. Note that for Cu-alloyed Ti-Ni-B2-phase no experimental data are available. As a first approximation we set the Cu-related ordering contributions to diffusivities of (metastable) binary Cu-Ti and Cu-Ni compounds of this phase to the same values as for the Ti-Ni compound. Assessed diffusivities of the ordered austenitic SMA matrix phase are used for the numerical solution of energy dissipation during precipitation, a pre-requisite of predictive simulation of the precipitate evolution discussed in the following section.



Figure 3. Calculated interdiffusion in the B2-ordered austenitic TiNi phase. Experimental data (symbols) from Divinski et al. [28] are included

3.3. Precipitate evolution in Ti-Ni and Cu-alloyed Ti-Ni SMA

Thermodynamic calculations of individual composition-temperature states, obtained by using the assessed Ti-Ni-Cu database allow pre-definitions of proper heat-treatments for controlled precipitation already prior to kinetic simulation. Computational thermodynamics suggest negligible formation of intermetallic precipitates in Ti50Ni50- χ Cu χ , $\chi < 0.2$. At $\chi > 0.2$ a significant equilibrium fraction of Ti_2Ni and tau1 was calculated at temperatures below 280°C . As a consequence in Ti50-Ni25-Cu25 (TI50CU25) the temperature of full solid solution treatment to form single B2-phase was strongly increased (680°C) relative to TI50CU20 (485°C). In both alloys intermetallic Ti-Cu phases and Ti_2Ni occurred. Ti-overstoichiometric Ti50.5CU25 revealed increased fractions of potential precipitate phases relative to TI50CU25 and allowed full solution treatment at 800°C . Second phase formation was negligible at a low temperature of 310°C for TI50CU20. Towards lower temperatures tau1 and Ti_2Ni became more stable. Testing composition deviations from equal atom fractions of Ti and (Ni+Cu) again, Ti-overstoichiometric Ti50.5CU20 represented an interesting composition in regard of solution treatment and precipitation. While being almost fully solution-treatable at 870°C (0.01 mol.% Ti_2Ni) the Ti_2Ni -stability was strongly increased relative to Ti50Ni30 (at 500°C 3 mol.% Ti_2Ni). On the other hand in TI49CU20 tau2 -phase formation was strongly increased, but this alloy would not be solution-treatable towards high temperatures. After these initial equilibrium consideration predictive (all kinetic calibration parameters in MatCalc kept default) isothermal thermo-kinetic precipitation simulations for potentially precipitation-strengthened TI50Cu25, TI50.5CU25, TI50CU20 and TI50.5CU20 were performed stepwise from high to low temperatures. From our equilibrium pre-investigation we identified intermetallic phases occurring in those compositions and considered Cu_4Ti_3 , CuTi , Ti_2Cu , Ti_2Ni as potential precipitates. The resulting isolines of 10% precipitate fractions relative to maximum fraction are presented in the time-temperature-precipitation (TTP)-diagrams of Fig. 4. Isothermal aging steps with relevant precipitation were inserted to show absolute precipitate fractions in mol.%.

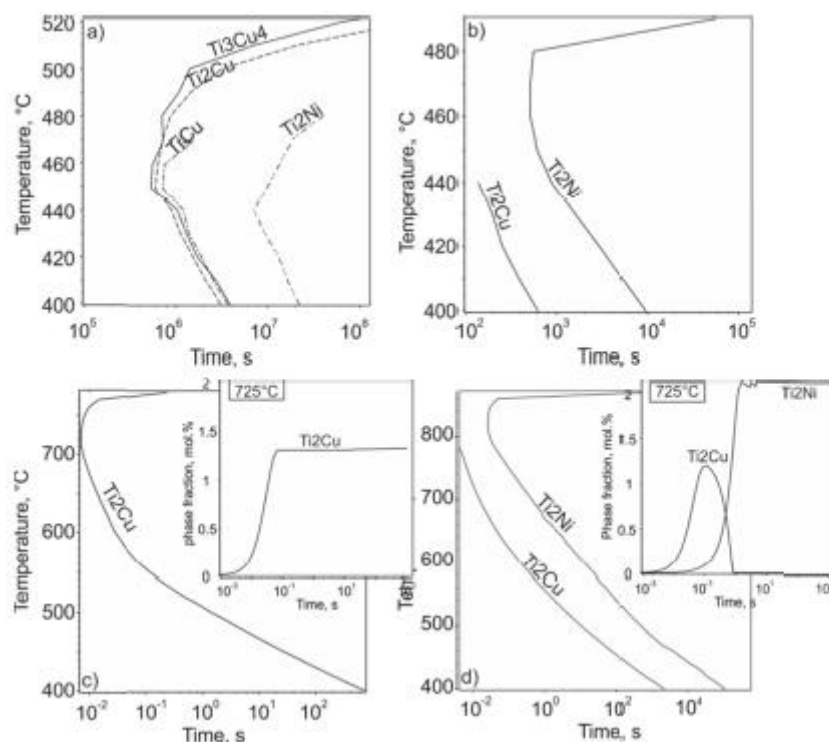


Figure 4. Simulated time-temperature-precipitation in TI50CU25 (a), TI50CU20 (b), TI50.5CU25 (c) and TI50.5CU20 (d)

The TTP-diagrams confirmed that the chosen Ti-overstoichiometry (c, d) shifted the start of precipitation towards higher temperatures and shorter aging times. The inserts in Fig. 5 (c, d) reveal a significant fraction of precipitates at the TTP-nose in TI50.5CU20 and TI50.5CU25, whereas precipitation in the TI50-variants (a, b) took too long to be of technological strengthening interest (TI50CU25), or was too weak (TI50CU20). In TI50.5CU25, Ti₂Cu dominated, with precipitation starting around 780°C. Nucleation and growth at this temperature was rapid. At 400°C, the 10 % isoconcentration line was crossed after approx. 10 minutes of aging. Ti₂Ni was the first precipitate to form in TI50.5CU20 at a high temperature with its TTP-nose around 850°C. Towards lower temperatures, Ti₂Cu was precipitating prior to Ti₂Ni. As in TI50.5CU25, kinetics became slower with decreasing temperatures, likely allowing better control of nucleation and growth during technological heat treatments: At 500°C, the 10 % iso-concentration line of Ti₂Cu was crossed after approx. 10 minutes of aging.

For high-performance SMA, there is demand of combining single-step martensitic B2 to B19 transformation at relatively high temperatures with precipitation strengthening. This, in turn requires the examination of B2-matrix composition modulated by precipitation. Interestingly, calculated *T₀*-temperatures (the highest theoretic temperature for the start of martensitic transformation, where *G_m*(B2-austenite) equals *G_m*(martensite) with the same composition) of TI50.5CU25 and TI50.5CU20 altered by precipitation were increased by 40°C and 20°C, respectively, relative to the TI50 variants.

Our simulation results thus indicate that an alloy composition between T50.5CU20 and T50.5CU25 may be a promising choice for both optimal martensitic transformation behavior and precipitation strengthening.

4. Conclusion

Based on CALPHAD-assessed thermodynamic and diffusion mobility databases, the kinetics of precipitation in Ti-Ni-Cu SMA was evaluated. Ti₂Ni and metastable Ti₂Cu were identified as most important precipitation phases. Computational thermodynamics confirmed that the martensitic transformations strongly depend on the amount of Cu-alloying. For single-step transformation associated with minimal transformation hysteresis, and thus optimal shape memory effect our calculation suggests alloying with Cu above approx. 15 at.%. Precipitation took place under strong control of alloying. Precipitation could change the mean matrix composition and associated martensite transformation temperature significantly. Our simulations suggest alloying of Cu from 20 to 25 at.% for precipitation strengthening in balance with high relatively martensite transformation temperatures. Slight Ti-overstoichiometric nominal composition (Ti around 50.5 at.%) increases precipitate fraction of Ti₂Ni and/or Ti₂Cu during aging of solution-treated SMA. Computational simulations with our compiled thermodynamic and diffusion mobility databases, combined with precipitate nucleation and growth models are suitable for defining ingenious heat treatments for advanced SMA performance.

References

- [1] Buehler, W J; Gilfrich, J W; Wiley, R C 1963 *J. Appl. Phys.* **34** 1475
- [2] Otsuka, K.; Ren, X. 2005 *Prog. Mater. Sci.* **50** 511
- [3] Khalil-Allafi, J, Ren, Xy; Eggeler, G 2002 *Acta Mater.* **50** 793
- [4] Khalil-Allafi, J; Eggeler, G; Schmahl, W, Sheptyakov, D 2006 *Mater. Sci. Eng. A-Struct Mater. Prop. Microstruct. Process.* **438-440** 593
- [5] Akin, E. 2010, Thesis, Texas A&M University.
- [6] Moberly, W J; Proft, J L; Duerig, T W; Sinclair, R. 1990 *Mater. Sci. Forum* **56-58** 605
- [7] Nam, T H; Saburi, T; Shimizu, K 1990 *JIM* **31** 959
- [8] Fukuda, T; Kitayama, M; Kakeshita, T; Saburi, T 1996 *Mater. Trans. JIM* **37** 1540

- [9] Cesari, E; Pons, J; Santamarta, R; Segui, C; Stroz, D; Morawiec, H In: Morawiec H, Stroz D, editors. Proc XVIII Conference on Applied Crystallography. Singapore: World Scientific; 2001. p. 171
- [10] Kaufmann, L; Bernstein, H 1970 *Academic Press*, New York
- [11] Saunders, N; Miodownik, A P 1998 *Calphad Calculation of Phase Diagrams. Pergamon Materials Series 1* Elsevier Science Ltd.
- [12] Povoden-Karadeniz, E; Cirstea, D C; Lang, P; Wojcik, T; Kozeschnik, E 2013 *CALPHAD* **41** 128
- [13] Tang, W; Sandstrom, R; Myazaki, S 2000 *J. Phase Equilib.* **21** 227
- [14] Zhang, H; He, Y; Yang, F; Liu, H; Jin, Z 2013 *Thermochim. Acta* **574** 121
- [15] Van Loo, V J J; Bastin, G F; Leenen, A J H 1978 *J. Less-Common Metals* **57** 111
- [16] <http://matcalc.tuwien.ac.at/>. Author: Kozeschnik, E. Last date of access: 2014-12-01; current MatCalc version is 5.61.057.
- [17] Wang, J; Liu, C.; Leinenbach, C.; Klotz, U. E.; Uggowitzer, P. J.; Löffler, J. F. 2011 *CALPHAD* **35** 82
- [18] an Mey, S. 1992 *CALPHAD* **16** 255.
- [19] Ansara, I; Dupin, N; Lukas, H.L; Sundman, B. 1997 *J. Alloys Cmpd.* **247** 20
- [20] Dinsdale, A T 1991 *CALPHAD* **15** 317
- [21] Volmer, M; Weber, A. 1926 *Z. Phys. Chemie* **119** 277
- [22] Svoboda, J; Fischer, F D; Fratzl, P, Kozeschnik, E 2004 *Mater. Sci. Eng. A-Struct. Mater. Prop. Microstruct. Process.* **385** 166
- [23] Onsager, L 1931 *Phys. Rev.* **37** 405
- [24] Onsager, L 1931 *Phys. Rev.* **38** 2265
- [25] Svoboda, J; Turek, I; Fischer, F D 2005 *Philos. Mag.* **85** 3699
- [26] Kozeschnik, E; Janssens, K; Bataille, C 2012 *Modeling Solid-State Precipitation. Momentum Press*, New York.
- [27] Helander, T; Agren, J 1999 *Acta Metal.* **47** 3291
- [28] Divinski, S V; Stloukal, I; Kral, L; Herzig, C 2009 *Defect Diffusion Forum* **289-292** 377

Cesari E, Pons J, Santamarta R, Segui
 C, Stroz D, Morawiec H.